Microbiological Research 292 (2025) 127997

Contents lists available at ScienceDirect

Microbiological Research

journal homepage: www.elsevier.com/locate/micres

Listeria monocytogenes colonises established multispecies biofilms and resides within them without altering biofilm composition or gene expression

Eva M. Voglauer [a,*], Lauren V. Alteio [a], Nadja Pracser [a], Sarah Thalguter [a], Narciso M. Quijada [b], Martin Wagner [a,c], Kathrin Rychli [c]

[a] FFoQSI GmbH – Austrian Competence Centre for Feed and Food Quality, Safety and Innovation, Technopark 1D, Tulln 3430, Austria
[b] Institute for Agribiotechnology Research (CIALE), Department of Microbiology and Genetics, University of Salamanca, Villamayor 37185, Salamanca, Spain
[c] Centre for Food Science and Veterinary Public Health, University of Veterinary Medicine Vienna, Veterinaerplatz 1, Vienna 1210, Austria

ARTICLE INFO

Keywords:
Listeria monocytogenes
Biofilm
Transcriptome
Pseudomonas fragi
Brochothrix thermosphacta
Carnobacterium maltaromaticum
Stainless steel

ABSTRACT

Listeria (*L.*) *monocytogenes* can survive for extended periods in the food producing environment. Here, biofilms possibly provide a niche for long-term survival due to their protective nature against environmental fluctuations and disinfectants. This study examined the behaviour of a *L. monocytogenes* ST121 isolate in a multispecies biofilm composed of *Pseudomonas* (*P.*) *fragi*, *Brochothrix* (*B.*) *thermosphacta*, and *Carnobacterium (C.) maltaromaticum*, previously isolated from a meat processing facility. The composition of the biofilm community and matrix, and transcriptional activity were analysed. *L. monocytogenes* colonised the multispecies biofilm, accounting for 6.4 % of all total biofilm cells after six hours. Transcriptomic analysis revealed 127 significantly upregulated *L. monocytogenes* genes compared to the inoculum, including motility, chemotaxis, iron, and protein transport related genes. When comparing the differentially expressed transcripts within the multispecies biofilm with and without *L. monocytogenes*, only a cadmium/zinc exporting ATPase gene in *C. maltaromaticum* was significantly upregulated, while the other 9313 genes in the biofilm community showed no significant differential expression. We further monitored biofilm development over time (6, 24 hours and 7 days). *P. fragi* remained the dominant species, while *L. monocytogenes* was able to survive in the multispecies biofilm accounting for 2.4 % of total biofilm cells after 7 days, without any significant changes in its abundance. The presence of *L. monocytogenes* did neither alter the biofilm community nor its matrix composition (amount of extracellular DNA, carbohydrates, and protein). Our data indicate that *L. monocytogenes* resides in multispecies biofilms, potentially increasing survival against cleaning and disinfection in food processing environments, supporting persistence.

1. Introduction

Microorganisms in natural and built environments predominantly live in communities protected by a self-produced matrix of extracellular polymeric substances (EPS). Within these so-called biofilms, the microbial cells show altered phenotypes and gene expression patterns compared to their planktonic counterparts. Furthermore, the self-produced shared matrix acts as protective shield, nutrient resource, and provides room for genetic exchange (Flemming et al., 2022). Environmental stresses, such as unfavourable growth temperatures, salinity, starvation or desiccation, have been shown to favour biofilm formation (Kubota et al., 2008; Mah and O'Toole, 2001). Biofilms develop on surfaces with and without experiencing shear stress (Carrascosa et al., 2021) and on surfaces of liquids (Flemming et al., 2016). All these conditions are encountered in the food processing environment (FPE).

Biofilms serve as protective strategy for bacteria to survive harsh environmental conditions as well as rigorous cleaning and disinfection strategies. In the context of food production, biofilms are seen as a source for food contamination with spoilage bacteria, food-borne pathogens or their quality-disturbing metabolites (e.g. toxins, enzymes)(Giaouris and Simões, 2018). In addition, enormous economic

* Corresponding author.
E-mail address: eva.voglauer@ffoqsi.at (E.M. Voglauer).

https://doi.org/10.1016/j.micres.2024.127997
Received 7 October 2024; Received in revised form 29 November 2024; Accepted 3 December 2024
Available online 11 December 2024

costs arise due to the need for biofilm control strategies including daily maintenance of safe food production (Cámara et al., 2022). Research showed that bacteria are omnipresent along the production line with product, and facility-specific occurrence of bacteria (Bokulich and Mills, 2013; Fox et al., 2014; Quijada et al., 2018), and transmission within the facility (Zwirzitz et al., 2020). Yet, certain genera are shared among most types of FPE, including *Pseudomonas*, *Acinetobacter*, *Staphylococcus*, *Psychrobacter*, *Stenotrophomonas*, *Serratia* and *Microbacterium* (Xu et al., 2023). Members of these genera were already characterised as biofilm-formers under monospecies conditions (Tang et al., 2013; Wagner et al., 2021), or were shown to have spoilage capacities (Maes et al., 2019).

Food contamination with spoilage and/or pathogenic bacteria is a serious issue in today's food production systems. According to the World Health Organization, 420,000 deaths are caused each year due to contaminated food (Food-Borne Disease Burden Epidemiology Reference Group, 2007-2015, 2015). Among the microorganisms causing foodborne diseases, *Listeria* (*L.*) *monocytogenes* is of great concern due to high hospitalisation and fatality rates, especially in vulnerable groups. The consumption of *L. monocytogenes*-contaminated food can lead to the infectious disease listeriosis, which is especially dangerous for immunocompromised and elderly people, pregnant women and their fetuses. Although in today's food production *L. monocytogenes* is actively managed via routine testing strategies, and cleaning and disinfection cycles, it is still able to persist in FPE for years (Belias et al., 2022; Fagerlund et al., 2016; Harrand et al., 2020). This long-term survival in FPE is thought to be facilitated in part by the presence of biofilms, which may harbour and support the persistence of this pathogen.

Laboratory experiments demonstrated that *L. monocytogenes* is able to form monospecies biofilms on various surfaces (glass, plastics, stainless steel) (Blackman et al., 1996; Gray et al., 2021). In addition is has been shown that biofilms are able to transfer living cells to food products (Truelstrup Hansen and Vogel, 2011). *L. monocytogenes* biofilms vary in structure from knitted chains (Rieu et al., 2008) to honeycomb-like morphotypes (Guilbaud et al., 2015). The transcriptome of *L. monocytogenes* during early stages of monospecies biofilm formation (after 24 and 48 h, 14 °C) was previously described (Gray et al., 2021), showing increased expression of genes related to transport, energy production and metabolism during initial colonisation stages.

Yet, in real-life scenarios multispecies biofilms are present rather than monospecies biofilms (Diaz et al., 2025; Maes et al., 2017; Pracser et al., 2024; Wagner et al., 2020). It was shown that *L. monocytogenes* benefits from protection by other bacteria resulting in increased tolerance to benzalkonium chloride (Rolon et al., 2024). Further it is able to regrow after disinfection with sodium hypochlorite and peracetic acid in multispecies biofilms (Fernández-Gómez et al., 2023). The presence of *Listeria* within biofilms in FPE was recently confirmed for the first time in a frozen vegetable environment (Pracser et al., 2024). Until then, only descriptive studies indicated the co-presence of *Listeria* with its accompanying microbiota without confirmed biofilm presence. Data regarding *Listeria*-associated microbiota show differences between the studies and are partially contradictive (Fagerlund et al., 2021; Liu et al., 2016; Pracser et al., 2024; Rodríguez-López et al., 2015; Zwirzitz et al., 2021). There is gathering evidence that *Listeria* can occur with diverse microbiota, which are different in the specific FPE. It remains unclear whether *L. monocytogenes* can colonise existing biofilms created by other bacterial species, and to what extent its presence influences the surrounding microbial community. There is limited literature available, suggesting the co-occurrence of *Listeria* with certain genera (Fagerlund et al., 2021) under real food production conditions (Pracser et al., 2024; Zwirzitz et al., 2020). Detailed analysis of *L. monocytogenes* behaviour in food-related multispecies biofilms is still lacking.

In this study, we tested if *L. monocytogenes* is able to colonise a multispecies biofilm composed of *Brochothrix* (*B.*) *thermosphacta*, *Carnobacterium* (*C.*) *maltaromaticum*, and *Pseudomonas* (*P.*) *fragi*, which were previously isolated from multispecies biofilms in a single meat processing environment (Wagner et al., 2020). Moreover, these three species have been described to be associated with *L. monocytogenes* presence (Fagerlund et al., 2021). The selected *L. monocytogenes* strain belongs to sequence type (ST) 121 and was repeatedly isolated from this meat processing facility (Stessl et al., 2020), but its biofilm forming ability has not yet been investigated. Biofilm growth under FPE conditions was mimicked on a food-relevant surface (stainless steel), under low temperature (10 °C), and using a limited but repeated nutrient supply (0.1-diluted tryptic-soy-broth supplemented with yeast extract). After growing a multispecies biofilm for 24 h, we introduced the *L. monocytogenes* strain and investigated the biofilm composition and gene expression after 6 h. In addition, we explored biofilm development with and without *L. monocytogenes* over time (6 h, 24 h and 7 days) by analysing the biofilm community structure and matrix composition (carbohydrates, extracellular DNA, and proteins). This study provides insights into the colonisation behaviour of *L. monocytogenes* within a multispecies biofilm.

2. Material and Methods

2.1. Strains and genomes

All strains were collected from a single Austrian meat processing facility (Table 1). The strains were stored in 30 % glycerol stocks at −80 °C. Cultures were streaked out on tryptic soy agar supplemented with yeast extract (TSA-Y) and incubated for 48 h at 20 °C or 37 °C for *L. monocytogenes*.

Genomes of *B. thermosphacta*, *C. maltaromaticum* and *P. fragi* strains were previously sequenced (Table 1; Wagner et al., 2021). For genome sequencing of the *L. monocytogenes* strain AU5961 (Linage II, ST121), one bacterial colony was inoculated in 4 ml of tryptic soy broth (TSB) supplemented with yeast extract (Y) and incubated for 16 h at 37 °C, 150 rpm shaking. DNA was isolated using the GeneJET Genomic DNA Purification Kit (Thermo Scientific). Genome sequencing was performed using Illumina MiSeq sequencing technology (300 bp length paired-end sequencing) (Microsynth, Balgach, Switzerland).

2.2. Biofilm model

A previously developed static biofilm model was used in this study (Wagner et al., 2021). To study the behaviour of *L. monocytogenes* in a multispecies biofilm set-up, three different types of biofilms were compared: multispecies (MS) biofilms without *L. monocytogenes* (MS-Lm), multispecies biofilms with *L. monocytogenes* addition (MS+Lm) and monospecies *L. monocytogenes* biofilms (Lm) (Fig. 1).

These biofilms were analysed at three different time points (6 h, 24 h and 168 h). To ensure similar starting conditions, their inocula were investigated (Supplementary Tables S1 and S2/Fig. 2). Fig. 1 gives a simplified overview about the different experimental set-ups and was created in BioRender (Voglauer, E. (2024) BioRender.com/m88u736). Supplementary Table S3 gives a detailed overview about the experimental set-up. The used stainless steel slides were immersed in the media-cell suspension leading to a potential biofilm-growth area of 16.46 cm^2.

In detail, one colony each of the *P. fragi*, *B. thermosphacta* and *C. maltaromaticum* strains was inoculated in 1:2 diluted TSB-Y and grown for 16 h at 20 °C (shaking 100 rpm). Sterile stainless steel slides were inserted in 1:10 diluted TSB-Y (final volume 60 ml). The medium was inoculated using overnight cultures of the *P. fragi*, *B. thermosphacta* and *C. maltaromaticum* strains in an equal ratio (optical density (OD_{600}) 0.1), equal to log CFU/ml 4.6–5.1 (Supplementary Table S1). The stainless steel slides were incubated at 10 °C for 24 h with shaking, resulting in a multispecies biofilm (time point 0).

In parallel, one *L. monocytogenes* colony was inoculated in 1:2 diluted TSB-Y and grown at 37 °C for 8 h (shaking 100 rpm) and adapted at 10 °C for 16 h without shaking. On the inoculation day, this culture was

Table 1
Strains used in this study.

Species	Strain ID	Isolation source	Year	Reference	PATRIC ID	NCBI BioSample ID
Brochothrix thermosphacta	BF1	Tumbling room: cutter wagon (FCS)	2018	(Wagner et al., 2020)	2756.50	SAMN18354422
Carnobacterium maltaromaticum	BF1	Tumbling room: screw conveyor (FCS)	2018	(Wagner et al., 2020)	2751.409	SAMN18354423
Pseudomonas fragi	BF1	Filling room: screw conveyor (FCS)	2018	(Wagner et al., 2020)	296.63	SAMN18354427
Listeria monocytogenes	AU5961	Tumbling room: drain (NFCS)	2013	(Stessl et al., 2020)	1639.14404	SAMN41725359

Strains used in the present study collected in a meat processing facility. FCS = Food contact surface, NFCS = Non-food contact surface.

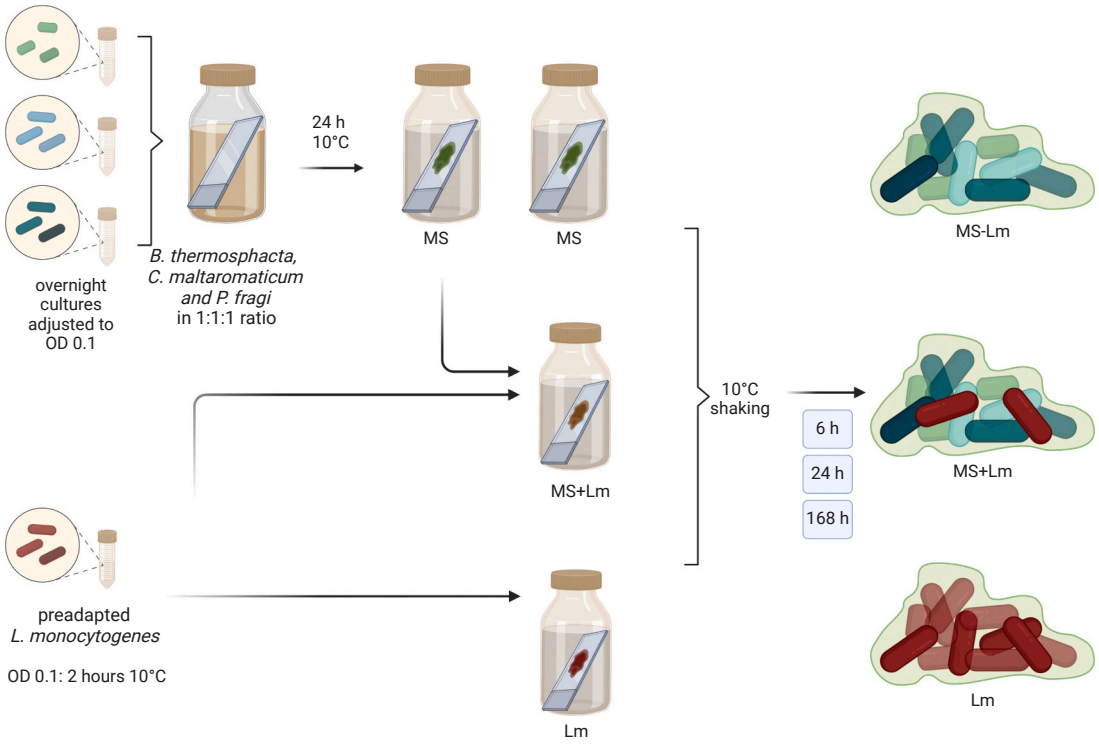

Fig. 1. Biofilm set-up. Multispecies biofilms consisting of *B. thermosphacta*, *C. maltaromaticum and P. fragi* were grown on stainless-steel slides [16.46 cm^2 immerged in media] at 10 °C in 1/10 TSB-Y after inoculation with overnight cultures in similar cell ratios. After 24 h these biofilms were either further cultivated (MS-Lm) or preadapted *L. monocytogenes* (already cultivated at 10 °C within the same media) were added (MS+Lm) at time point 0. Furthermore, the *L. monocytogenes* inoculum was used to set-up *Listeria*-only biofilms (Lm). The biofilms were incubated further for 6 h, 24 h or 168 h and subsequently harvested and analysed. Multispecies biofilms are always 24 h older than the *Listeria*-only biofilms, yet only the *Listeria*-only age is given in the different time points/figures due to reasons of clarity. Created in BioRender. Voglauer, E. (2024) BioRender.com/m88u736.

adjusted to an OD_{600} of 0.1 in 1:10 diluted TSB-Y two hours (10°C, 100 rpm) before addition to the multispecies biofilm (mean cell densities of 6.5 log CFU/ml, Supplementary Table S1).

The *Listeria*-only biofilms were started at this time point using the prepared *L. monocytogenes* culture. Replicates of four were prepared for each set-up at three different time points. Two of these biofilms were used for quantification of biofilm cells and the other two biofilms were used for matrix analysis.

After two hours, the biofilms were washed using 0.9 % NaCl solution and put into fresh media (TSB-Y 1:10). This step was repeated after 24 h, and 144 h. All media and solutions were pre-cooled to 10 °C. All incubation steps were performed at 10 °C with 100 rpm shaking, if not stated otherwise.

At each time point, two technical replicates were grown for the quantitative community analysis and biofilm matrix investigation, respectively. For the transcriptome study (6 h time point), ten slides of each type were pooled to increase biomass. All experiments were conducted three times.

For each time point a negative control was included: the stainless steel slide without intentional bacteria addition. All negative controls showed negative qPCR and matrix results.

Biofilms were harvested after 6 h, 48 h and 168 h. Each slide was washed using 0.9 % NaCl solution and harvested using glass beads (4 mm diameter) in 10 ml 0.1x PBS for matrix analysis and DNA quantification or RNA later (25 mM sodium citrate, 10 mM EDTA, 70 g ammonium sulphate/100 ml, pH = 5.2) for RNA extraction. The slides were inserted in the solution and vortexed for 3 minutes. The liquid was stored at −20 °C until further use, in case of DNA and RNA extraction. For matrix extraction the solution was treated with 2 g cation exchange resin as described in Wagner et al. (2020) and the collected matrix solution was stored at −20 °C until further analysis.

2.3. DNA and RNA extraction

DNA and RNA were extracted using the AllPrep® Power Fecal DNA/RNA Kit (QIAGEN) according to manufacturer's instructions. Lysis of the samples was done using FastPrep-24 5 G (MP Biomedicals) [settings: 5 × 45 seconds at 4.5 speed using dry ice]. Elution was carried out using two times 15 µl DEPC-H_2O, (70 °C pre-heated for DNA). A kit negative control was included in each extraction. The concentration was determined using 1 µl DNA and the spectrophotometer/Fluorometer DS-11 FX+ (DeNovix Inc., Wilmington, DE).

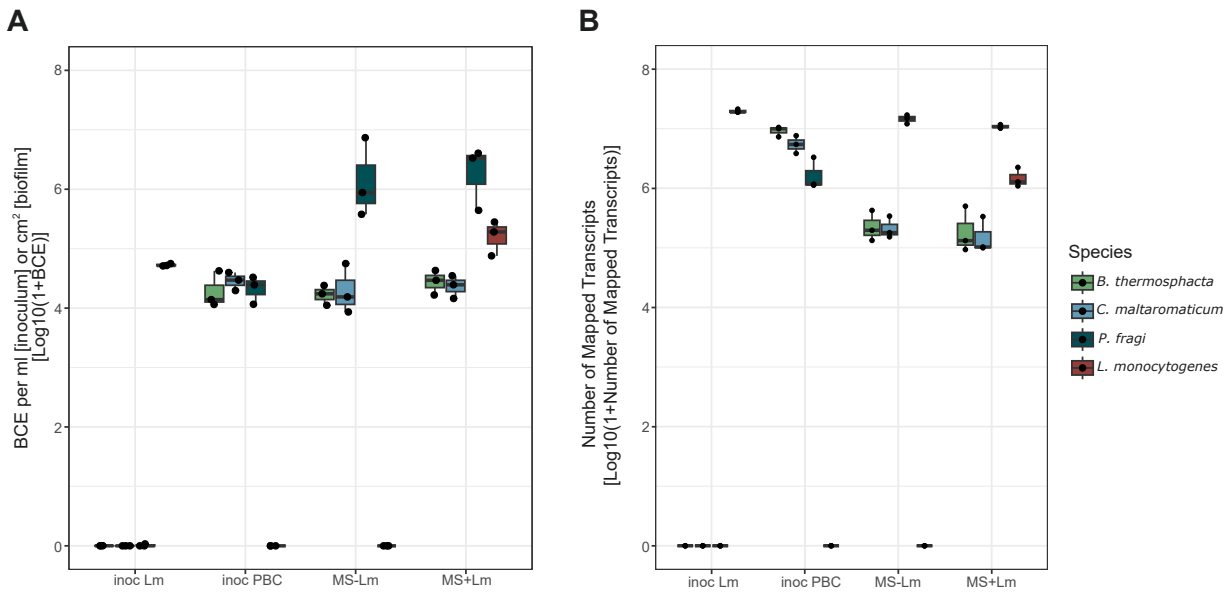

Fig. 2. Community composition and activity in the biofilm. BCE (A) and Log-transformed number of mapped transcripts (B) for each species in the *L. monocytogenes* inoculum (inoc Lm), the *Pseudomonas-Brochothrix-Carnobacterium* multispecies inoculum (inoc PBC), the multispecies biofilm without (MS-Lm) and with *L. monocytogenes* (MS+Lm); (n = 3 per group). Each biofilm had a potential growth area of 16.46 cm^2 on the stainless steel slide.

2.4. Quantitative evaluation of biofilm communities using qPCR

Strain-specific qPCR protocols were established to enumerate the respective number of cells for *P. fragi*, *B. thermosphacta* and *C. maltaromaticum* (Supplementary Table S4). For *L. monocytogenes*, a published probe-based qPCR approach was used (Rossmanith et al., 2006).

To validate these qPCR protocols and exclude possible cross-targeting of the primers test qPCRs were performed. Therefore, bacterial DNA of a pure overnight culture was isolated using the GeneJET PCR purification Kit (Thermo Fischer) following the provided instructions. The DNA concentration was determined using the Qubit 2.0 Fluorometer. The quantitative PCR assays were conducted using the 2x Agilent Brilliant III SYBR Green master mix (Agilent), except for *L. monocytogenes*, which was quantified by detecting the *prfA* gene, targeted by a specific probe (Rossmanith et al., 2006).

The sequences of the different primer pairs, reaction mixtures and cycling protocols are described in Supplementary Table S12. All qPCR assays were performed on Mx3000P qPCR thermocyclers, analysed with MxPro v.4.10 (Stratagene, San Diego, USA), all samples were analysed in duplicates and negative controls were included. Standard curves were produced using purified DNA from 10 mg/L to 1 000 000 mg/L, (as described in Dixon et al., 2019) [$R^2 > 0.99$; efficiency > 90 %]. All samples were analysed by qPCR in duplicates and negative controls for the extraction, as well as in each qPCR run were included. To exclude contamination bias we quantified the total 16S rRNA numbers (Supplementary Table S5, Supplementary Table S6), which were in line with the species-specific bacterial cell equivalent numbers.

2.5. Analysis of biofilm matrix: Carbohydrate, eDNA and protein analysis

The collected matrix was frozen at −20 °C until further analyses. Three different components of the matrix were determined: The total carbohydrates (glucose equivalents), the extracellular DNA levels and the protein abundance.

The carbohydrates, measured as total glucose equivalents, were determined after evaporation to increase the concentration using a previously described phenol-sulphuric acid plate assay (Wagner et al., 2020). The limit of quantification was 360 ng glucose per 50 µl.

The extracellular DNA (eDNA) levels were measured using the spectrophotometer/Fluorometer DS-11 FX+ (DeNovix Inc., Wilmington, DE) after precipitation (as described previously (Wagner et al., 2020)). The limit of detection was 0.75 ng/µl DNA.

The protein content was determined after precipitation and dissolving of the pellet in 25 mM TRIS-HCl pH 8 (originally described in Rychli et al., 2016 and adapted for matrix analysis according to Wagner et al., 2020). The content of proteins was determined using the Quant-iT kit following the provided instructions. Each sample was spiked using 250 ng BSA. A standard curve was used to calculate each sample value [minimal R^2 0.987]. The limit of blank (LOB) was determined by three independent measurements of eight negative control samples (ddH2O) following the protein precipitation protocol. The LOB was 404 ng, calculated according to Armbruster and Pry (2008).

2.6. Statistical analysis

Statistical analysis was performed in R v 4.3.3. (R Core Team, 2020) using RStudio v 2323.12.1. Data were tested for normal distribution using the Shapiro–Wilk normality test. The non-normally distributed groups were tested using the Wilcoxon-test for connected samples. Normally distributed data was tested using one-way ANOVA. Data were considered significant at $p \leq 0.05$. Plots were created using the package ggpubr (v 0.6.0.), which depends on ggplot2 (Wickham, 2016).

2.7. Transcriptomic analysis

2.7.1. RNA sequencing

The library preparation included quality control of total RNA samples, ribo-depletion with the Illumina Ribo-Zero Plus kit, cDNA synthesis and library preparation using barcodes as well as equimolar pooling according to library quantification measurements. Sequencing was done using Illumina NextSeq, v2.5, 20 M reads per sample (single end sequencing; 75 bp read length) (Microsynth, Balgach, Switzerland).

2.7.2. Preparation of reference genomes

Sequencing reads from reference strains were quality checked, quality filtered and assembled using “The Bacterial and Viral Bioinformatics Resource Center (BV-BRC)”, https://www.bv-brc.org/, using SPAdes v3.13.0. as assembly option. Contigs below 500 bp were removed. Assembly statistics were generated using QUAST (Gurevich

et al., 2013). The assembly of the *L. monocytogenes* reads yielded a genome length of 3096,483 bp in 34 contigs (L50: 3; N50: 451566). The assembled genome of *P. fragi* had a length of 5020,232 bp in 49 contigs (L50: 9; N50: 185374). Assembly of *B. thermosphacta* yielded a genome length of 2535,548 bp in 26 contigs (L50: 3; N50: 318207). *C. maltaromaticum* reads were assembled to a genome of 3479,071 bp in 24 contigs (L50: 2; N50: 355035).

All four reference genomes (*P. fragi* BF1, *B. thermosphacta* BF1, *C. maltaromaticum* BF1, *L. monocytogenes* AU5961) were merged into a single fasta file in order to mimic the reference metagenome of the multispecies biofilm. Coding sequences (CDS) and translated proteins were predicted using Prodigal v2.6.3 using the "meta" option. In total, 13,443 CDS were identified.

2.7.3. Transcriptomic analysis

Quality control of the sequencing raw reads was conducted by using FASTQC v.0.11.9. Adapter content was removed, and the reads were quality filtered using Trimmomatic (v0.39.; Bolger et al., 2014). All residual rRNA sequences were removed from the sequencing reads by using SortMeRNA (v4.3.4.; Kopylova et al., 2012). Between 2 % and 25 % of reads per sample were removed due to rRNA content. The processed reads were mapped against the merged reference genome file using Bowtie2 (v2.2.5.; Langmead and Salzberg, 2012). For each sample, the number of mapped reads per feature was calculated by FeatureCounts (v.2.0.1.; Liao et al., 2014a). Annotation of coding sequences was performed using DIAMOND v2.0.15 against the Kyoto Encyclopedia of Genes and Genomes (KEGG database, downloaded March 2021; Kanehisa et al., 2015) and the eggNOG database (downloaded August 2022; Huerta-Cepas et al., 2018). Additionally, annotation was performed using the NCBI non-redundant protein database (downloaded October 2023) with DIAMOND (v2.18.; Buchfink et al., 2021). Annotations were merged with the output of FeatureCounts (Liao et al., 2014b) and were further analysed for differentially expressed genes. In the *L. monocytogenes* inoculum, an average of 19.69 million filtered, rRNA-free reads mapped to the reference genome, representing 94.29 % of total reads mapping, indicating a good sequencing depth.

2.7.4. Differential gene expression analysis

Differential gene expression analysis was performed with DESeq2 (v1.38.3; Love and Anders, 2014) to compare gene expression of *L. monocytogenes*, as well as the multispecies biofilm community containing *Pseudomonas*, *Carnobacterium*, and *Brochothrix*, versus the inoculum. Additionally, differentially expressed genes (DEGs) were compared between the multispecies community in the presence of (MS+Lm) and without introduced *L. monocytogenes* (MS-Lm). Within each comparison, pre-filtering (removal of rows with gene counts < 10 in total) was conducted prior to differential gene expression analysis. Multiple test correction was performed using Benjamini-Hochberg to calculate adjusted p-values. The threshold for significantly DEGs included an adjusted p-value of ≤ 0.05 and log2 fold change ≥ 1.5 and a base mean of ≥ 20. Figures depicting differentially expressed genes were generated using ggplot2 (v3.5.1.; Wickham, 2016), ggpubr (v0.6.0; Kassambara, 2023), and ggsci (v3.0.0; Xiao, 2024) packages in R (v4.2.3.; R Core Team, 2020), (Supplementary Table S8).

2.7.5. Pathway enrichment analysis

Gene set enrichment analysis was performed on the KEGG pathways using the GAGE package in R (v2.48.0.; Luo et al., 2009). A q-value threshold of ≤ 0.05 was applied, and significantly up- and down-expressed pathways were visualized using ggplot2 (v 3.5.1.; Wickham, 2016). Gene set enrichment results for *L. monocytogenes* in the biofilm versus the inoculum, and for MS+Lm and MS-Lm biofilms versus the multispecies inoculum are available in the supplementary material (Supplementary Tables S7, S9–S13).

3. Results

3.1. Composition and transcriptional activity in the multispecies biofilm

Biofilms were grown on stainless steel slides in nutrient-depleted broth (10x diluted TSB supplemented with yeast extract) at 10 °C to mimic conditions in the FPE. The inoculum level of each species was equal for all three-species biofilms ranging from 4.3 to 4.5 log Bacterial Cell Equivalents (BCE) per ml inoculum (Fig. 2A). After 24 h of incubation, preadapted *L. monocytogenes* were added for 2 h to the biofilms with a mean bacterial count of 4.7 log BCE per ml inoculum (Fig. 2A). After additional 4 h the biofilms were harvested.

P. fragi was the most abundant species in the biofilm with 6.1 log BCE/cm^2, whereas *B. thermosphacta* and *C. maltaromaticum* counts reached only 4.2 and 4.3 log BCE/cm^2). *L. monocytogenes* was able to colonise the multispecies biofilm with cell numbers of 5.2 log BCE/cm^2 after 6 h. The presence of *L. monocytogenes* did not significantly change the abundance of *B. thermosphacta*, *C. maltaromaticum* and *P. fragi* in the biofilm (Fig. 2A).

In parallel, gene expression of each species in the inoculum and the established biofilm community was assessed by determining the number of transcripts from the entire community transcriptome that aligned to the reference genome of each of the different species (Fig. 2B). In the multispecies inoculum, *P. fragi*, *B. thermosphacta*, and *C. maltaromaticum* accounted for 10.04 % (log 6.05), 49.01 % (log 6.99), and 29.32 % (log 6.88) of the total number of transcript sequences, respectively. In comparison, the multispecies biofilm without *L. monocytogenes* (MS-Lm) revealed an average of 80.57 % (log 7.17) of reads mapping to *P. fragi*, while only 1.42 % (log 5.62) and 1.24 % (log 5.53) of transcripts mapped to *B. thermosphacta* and *C. maltaromaticum*. Similarly, in the multispecies biofilm with *L. monocytogenes* (MS+Lm) the multispecies community was dominated by *P. fragi*, with an average of 69.9 % (log 7.00) of transcripts mapping, while only 1.52 % (log 5.69) and 1.13 % (log 5.52) mapped to *B. thermosphacta* and *C. maltaromaticum*. Interestingly, an average of 9.72 % (log 6.34) of transcripts mapped to *L. monocytogenes* in the multispecies biofilm where it was introduced (Fig. 2B).

3.2. Gene transcription of Listeria monocytogenes

Pathway enrichment analysis comparing *L. monocytogenes* in the multispecies biofilm against its own inoculum revealed significant enrichment of pathways related to "Protein export" (ko03060), "Flagellar assembly" (ko02040), "Nitrogen metabolism" (ko00910), "Biosynthesis of amino acids" (ko01230), "Bacterial chemotaxis" (ko02030), "Two-component systems" (ko02020), "Alanine, aspartate and glutamate metabolism" (ko00250), "Bacterial secretion system" (ko03070), "Pyrimidine metabolism" (ko00240), "Biosynthesis of secondary metabolites" (ko01110), and "Biofilm formation – *Vibrio cholerae*" (ko05111) (Fig. 3). Most notably, "Biosynthesis of amino acids", "Two-component system", and "Biosynthesis of secondary metabolites" were the enriched pathways with the highest number of assigned genes. Enrichment analysis also revealed significant down-regulation of the pathways including "Porphyrin metabolism" (ko00860), "Biosynthesis of cofactors" (ko01240), and "Carbon metabolism" (ko01200), among others (Fig. 3).

Differential expression analysis of 3132 *L. monocytogenes* genes revealed 127 significantly up- and 277 significantly down-regulated transcripts in *L. monocytogenes* in the biofilm compared to the inoculum (Supplementary Figure 1). We investigated the top 50 up- and down- differentially expressed genes (DEGs) in *L. monocytogenes* in the MS+Lm biofilm compared to the *L. monocytogenes* inoculum (Supplementary Table S7, S8). Closer investigation of the specific genes revealed increased expression of genes related to "Amino acid transport and metabolism" (*gltD*, PRK06348, and *GlnQ*), "Inorganic ion transport" (*ugpA*, *emrE*, *metP*, *abcC*, *adcA*, *nlpA*, *ykaA*), "Nucleotide transport and

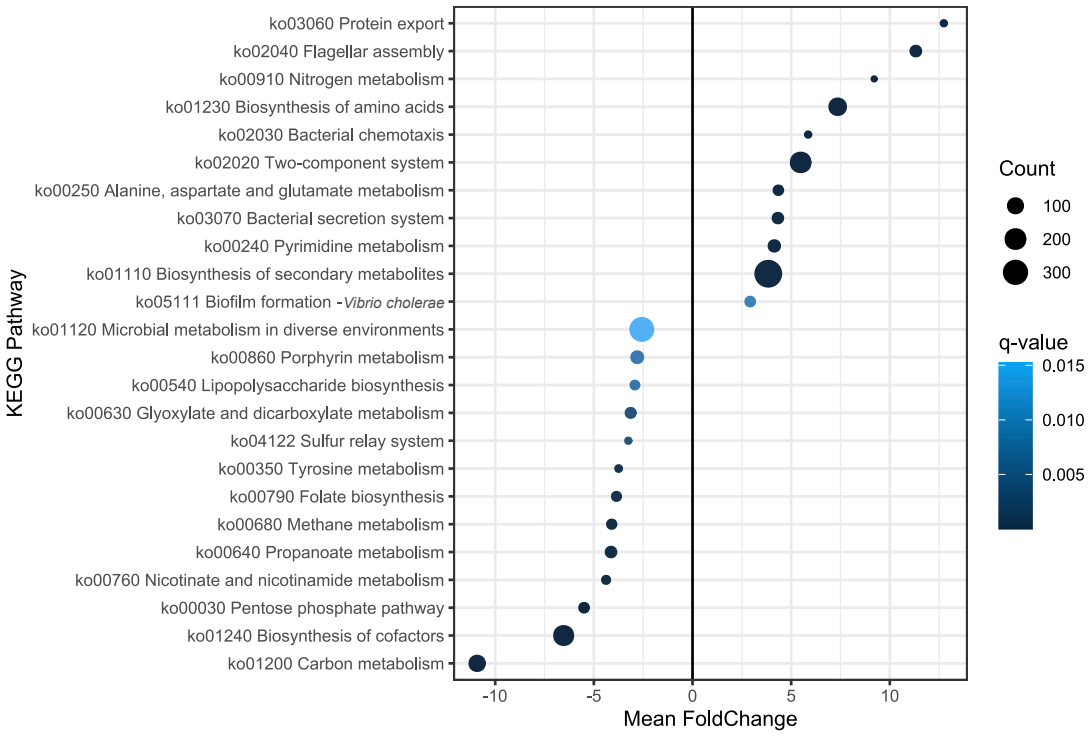

Fig. 3. Gene expression in *Listeria monocytogenes*. Pathway enrichment analysis for *L. monocytogenes* in the multispecies biofilm (MS+Lm) compared to the *L. monocytogenes* inoculum. Dots reveal the mean log-fold change for a given KEGG pathway. The size of each dot represents the number of genes contained within each pathway, and the color indicates the q-value. KEGG pathways indicated by koxxxxx can be searched online and detailed pathway schemes can be retrieved [https://www.genome.jp/dbget-bin/www_bget?pathway+koxxxxx].

metabolism" (PRK05205, PRK01117), "Transcription" (*deoR*, *tetR*_C_28, *cspC*, *rpiR*, *rnc*, *nusG*, penicillinase R, HTH MARR, *mngR*), and "Translation, ribosomal structure and biogenesis" (*rpsL*, PRK05302, *rplQ*, *rlmN*, *rluA*) (Table 2, Supplementary Table S7, S8, S9). Additionally, genes classified to the pathway "Extracellular Structures" were also significantly up-expressed, most notably phage Gp23. In six of the top 20 up-regulated genes no KEGG ID or function could be assigned (Table 2). The functions of the most expressed genes included: Transport genes (transpeptidase (*srtB*), iron (*ABC.FEV.S*), proteins (*tatA*)), chemotaxis (*motA*, *cheR*, *motB*), and motility (*flgG*, *flhA*, *flhB*). The most negatively

Table 2
Top 20 upregulated *L. monocytogenes* genes (multi-species biofilm versus inoculum).

#	name	lmo info	KEGG.ID	function	KEGG pathway(s)	log2 fold change	adjusted p-value
1	NA	unknown	unknown	unknown	unknown	4.09	0.0005
2	*srtB*	*lmo2181*	K08600	endopeptidase	Peptidases; Peptidoglycan biosynthesis and degradation proteins	4.09	0.0001
3	*motA*	*lmo0685*	K02556	chemotaxis	Two-component system; Bacterial chemotaxis; Flagellar assembly	3.97	0.0004
4	*cheR*	*lmo0683*	K00575	chemotaxis	Two-component system; Bacterial chemotaxis	3.91	0.0005
5	*ABC.FEV.S*	unknown	K02016	iron transport	unknown	3.75	0.0005
6	*tatA*	*lmo0362*	K03116	protein/iron transport	Protein export; Bacterial secretion system	3.71	0.009
7	NA	unknown	unknown	unknown	unknown	3.59	< 0.0001
8	*motB*	*lmo0686*	K02557	chemotaxis	Bacteral chemotaxis; Flagellar assembly	3.54	0.0012
9	NA	unknown	unknown	unknown	unknown	3.50	< 0.0001
10	*flgG*	*lmo0682*	K02392	motility - flagellum	Flagellar assembly	3.50	0.0008
11	*flhA*	*lmo0680*	K02400	motility - flagellum	Flagellar assembly	3.47	0.0009
12	*NA*	*lmo2280*	unknown	phage protein	unknown	3.27	< 0.0001
13	*NA*	*lmo1007*	unknown	unknown	hypothetical protein	3.26	0.0003
14	*flhB*	*lmo0679*	K02401	motility - flagellum	Flagellar assembly	3.26	0.0023
15	*pyrR*	*lmo1840*	K02825	transcriptional regulator	Pyrimidine metabolism; Metabolic pathways; Nucleotide metabolism	3.23	< 0.0001
16	*fliR*	*lmo0678*	K02421	motility - flagellum	Flagellar assembly	3.05	0.004
17	*NA*	unknown	NA	unknown	unknown	3.01	0.03
18	*cheV*	*lmo0689*	K03415	chemotaxis	Two-component system; Bacterial chemotaxis	2.96	0.02
19	*gltB*	*lmo0626*	K00265	glutamate synthase large chain	Alanine, aspartate and glutamate metabolism; Nitrogen metabolism; Metabolic pathways, Biosynthesis of secondary metabolites, Microbial metabolism a in diverse environments; Biosynthesis of amino acids	2.82	< 0.0001
20	*ABC.FEV.S*	unknown	K02016	iron transport	unknown	2.77	0.007

Unknown genes with *lmo* info were mapped against EGDe using NCBI database. *lmo2280* encodes a bacteriophage A118 related gene: Protein gp23. NA: not applicable

differentially expressed genes were assigned to EggNOG categories "Amino acid transport and metabolism" (M3B *PepF*, PRK06928, NADB Rossmann), "Carbohydrate transport and metabolism" (*celA*, PTS IIA, FBPase2, *glpF*), "Energy production and conversion" (PRK00784, *glpK*, MDR_like_2, *glpA*, ALDH_F5_SSADH_GabD), "Posttranslational modification, protein turnover, chaperones" (thioredoxin, *tpx*, *hslO*, *btuE*, thioredoxin_3, *clpA*), "Replication, recombination, and repair" (PRK05298, *uvrA*, RNase_HI_like), and "Signal transduction mechanisms" (*yesM*, *lytT*, *wzb*) (Supplementary Table S7, S9). It is important to note that many of the significantly up- and down-expressed genes were in the pathway categories "Function unknown", "General function prediction only", or could not be assigned to a pathway category ("NA").

3.3. Gene expression in the multispecies biofilm

The transcriptome of the multispecies biofilm with (MS+Lm) and

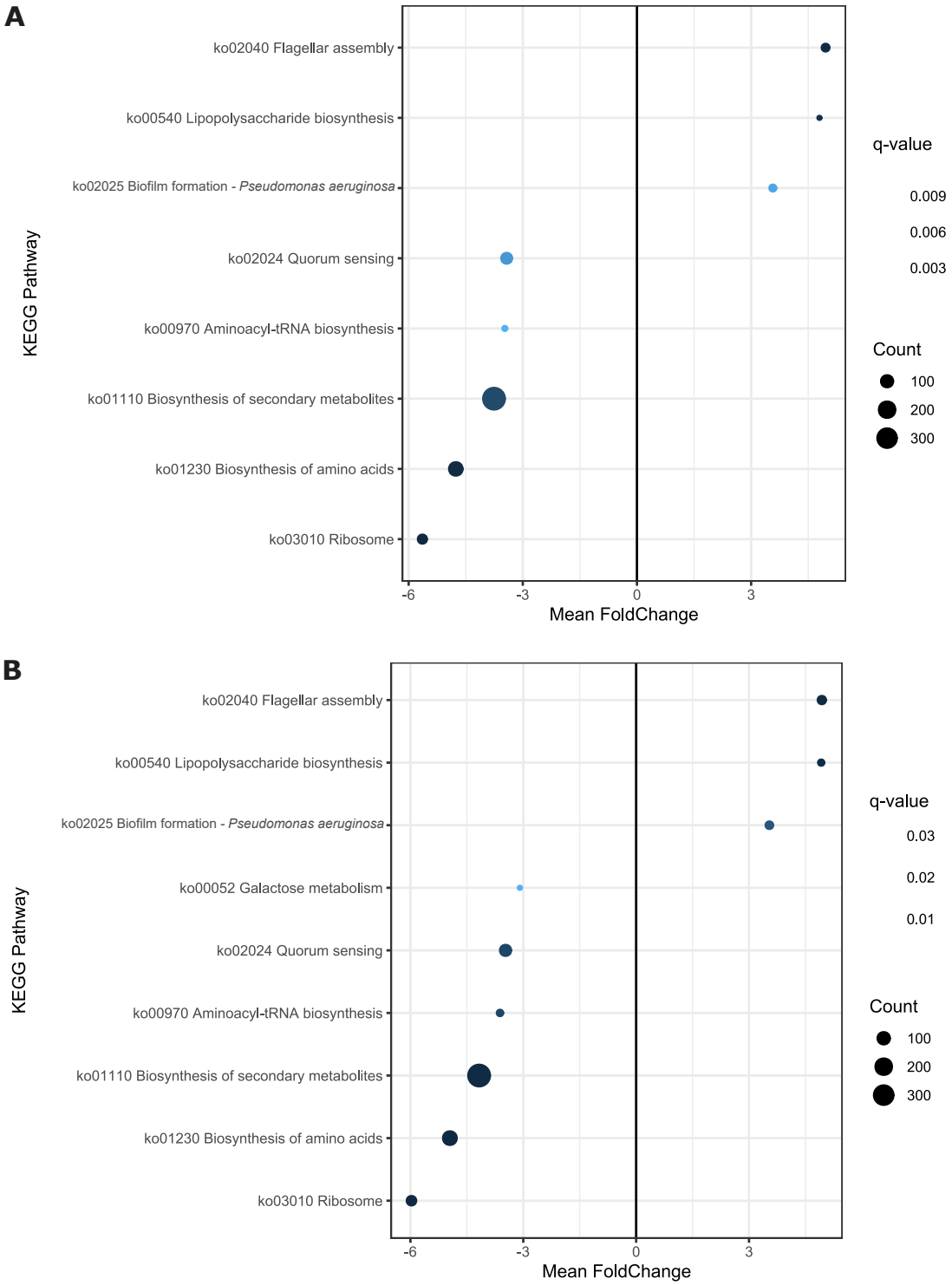

Fig. 4. Gene expression in multispecies biofilms. KEGG pathway enrichment analysis for the multispecies biofilm (A) with *L. monocytogenes* (MS+Lm) and (B) without *L. monocytogenes* (MS-Lm) as compared to the inoculum. KEGG pathways indicated by koxxxxx can be searched online and detailed pathway schemes can be retrieved [https://www.genome.jp/dbget-bin/www_bget?pathway+koxxxxx].

without *L. monocytogenes* (MS-Lm) was analysed to determine if the introduction of *L. monocytogenes* altered gene expression in the established biofilm community. Differential gene expression analysis revealed lower overall gene expression in MS+Lm when compared to the inoculum (Supplementary Figure 2), with 3700 transcripts up-regulted in MS+Lm compared to 4226 in MS-Lm. Comparison of the number of transcripts with a negative log2 fold change revealed similar results for MS+Lm and MS-Lm biofilms in comparison to the MS-inoculum, with 4790 and 4160 transcripts down-regulated respectively. In both the MS+Lm and MS-Lm biofilms, most up-expressed transcripts were assigned to *P. fragi* (3697 and 4195), whereas down-expressed transcripts were mostly assigned to *B. thermosphacta* (2207 and 1996) and *C. maltaromaticum* (2577 and 2162).

Interestingly, comparison of differentially expressed transcripts between the multispecies biofilm with and without *L. monocytogenes* revealed that only *zntA*, a cadmium/zinc exporting ATPase in *C. maltaromaticum*, was significantly up-regulated (log2 fold change=2.899, adjusted *p*-value=0.001). Of the 9314 genes analysed from the multispecies biofilm communities, the remaining genes were not significantly differentially expressed after multiple test correction according to the applied cut-off.

Pathway enrichment analysis was conducted to examine pathway-level changes in expression in the multispecies biofilms (MS+/- Lm) compared to the inoculum (Fig. 4). In the MS-Lm biofilm, transcripts related to "Flagellar assembly" (ko2040), "Lipopolysaccharide biosynthesis" (ko00540), and "Biofilm formation - *Pseudomonas aeruginosa*" (ko02025) were up-regulated relative to the multispecies inoculum. Pathway enrichment analysis also revealed the down-expression of pathways related to "Quorum sensing" (ko02024), "Amino-acyl tRNA biosynthesis" (ko00970), "Biosynthesis of secondary metabolites" (ko01110), "Biosynthesis of amino acids" (ko01230), and "Ribosome" (ko03010) in both the MS+Lm and MS-Lm treatments. In the MS-Lm, "Galactose metabolism" was also observed to be significantly down-regulated (ko00052), which was not observed in the MS+Lm biofilm community.

In both the MS+Lm and MS-Lm biofilms compared to the MS-inoculum, nine of the top 20 significantly up-regulated transcripts were shared, including *tonB*-dependent siderophore receptor (*fiu*), sensor histidine kinase (*baeS*), coA transferase subunit A (*atoD*), SDR family oxidoreductase (SDR_c5), cytochrome-c oxidase subunit IV (*fixQ*), *fecR* family protein, FUSC family protein, and one unknown gene (unknown_protein1406, ENOG410XUDB). Of the top 20 significantly down-expressed transcripts, five transcripts were similarly down-expressed in MS+Lm and MS-Lm biofilms compared to the inoculum, including heavy metal translocating P-type ATPase (*zosA, pfeT*-like), transporter substrate-binding protein (PBP2_UgPB), PBP2_OppA, carbohydrate ABC transporter permease (*ugpE*), and a hypothetical protein (unknown gene region 190) (Supplementary Tables S10-S13).

3.4. Bacterial community structure

Next, we wanted to explore the biofilm development with and without *L. monocytogenes* over time (Fig. 5, Supplementary Table S14). Multispecies biofilms were grown with and without *L. monocytogenes* on stainless steel slides at 10 °C, their composition was measured after 6 h, 24 h and 168 h (7 days). We additionally included a *Listeria*-only biofilm. After 24 h in the MS+Lm biofilm showed the maximum mean bacterial load per biofilm, which was 6.3 log BCE/cm^2 (detected via the 16S rRNA gene) (Supplementary Table S5).

P. fragi was the dominant species in the multispecies biofilms at all time points (Fig. 5). It accounted for over 90 % of all bacteria at 6 h (4.9 log BCE/cm^2) and 24 h and 70 % after 7 days. In multispecies biofilms without *L. monocytogenes* (MS-Lm), *B. thermosphacta* and *C. maltaromaticum* increased in their relative abundance over time: for *B. thermosphacta* from 0.2 (6 h) to 0.3 (24 h) to 8.3 % (168 h) and for *C. maltaromaticum* from 0.5 to 0.7 to 22.7 % (Supplementary Table S14, Supplementary Figure S2). *B. thermosphacta* numbers increased from 2.4 to 3.1 to 4.1 log BCE/cm^2 (statistically significant difference 6 h vs. 168 h, $p = 0.026$). *C. maltaromaticum* numbers were statistically significant different in 6 h vs. 168 h MS-minus biofilms, which was an increase from log 2.8 BCE/cm^2 to log 4.5 BCE/cm^2 ($p = 0.026$). There was no significant change in *P. fragi* counts between the timepoints (Fig. 5). *B. thermosphacta*, *C. maltaromaticum* and *L. monocytogenes* accounted for 9.7, 15.9 and 2.4 %, respectively in the MS+Lm biofilm after 7 days of incubation. Here, no significant changes in *P. fragi, B. thermosphacta* and *C. maltaromaticum* numbers could be observed over time. The highest number of *L. monocytogenes* relative to the other multispecies members was seen at the 6 h time point, constituting 5.3 % (3.3 log BCE/cm^2).

The biomass (mean BCE levels) of *L. monocytogenes* in *Listeria*-only biofilms increased from 2.5 log BCE/cm^2 at 6 h to to 4.1 log BCE/cm^2 (168 h). Compared to the multispecies biofilms, there was no statistical difference in *L. monocytogenes* numbers in *Listeria*-only biofilms and multispecies biofilms with *L. monocytogenes* (MS+Lm) at all time points (Fig. 5).

3.5. Biofilm matrix composition

In all biofilms we were able to detect eDNA, carbohydrates and proteins (Fig. 6). The amount of eDNA ranged from 36.2 ng/cm^2 (*Listeria*-only 24 h) to 340.9 ng/cm^2 (MS+Lm 7 days). We observed a trend that eDNA content increased over time.

The highest carbohydrate load was detected after 6 h in the MS-Lm biofilm (3.7 µg/cm^2), whereas the lowest amount after 24 h in the *Listeria*-only biofilm (2.3 µg/cm^2). There was a significant change in the

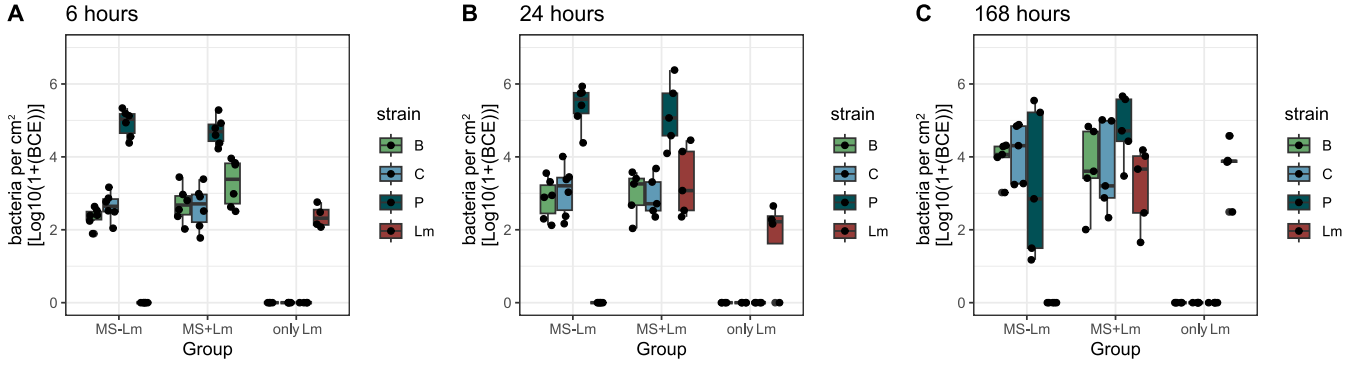

Fig. 5. Bacteria per biofilm. The numbers of bacteria (bacteria cell equivalents (BCE) as determined by strain-specific qPCR given per cm^2) are shown. Boxplots of the 6 h (A), 24 h (B) and 168 h (=7 days, C) summarize the different bacterial numbers in the different biofilm groups (MS-Lm, MS+Lm and only *Listeria*). The indicated timepoints represents the time after (theoretical) *L. monocytogenes* addition. Multispecies biofilms were already incubated for 24 h (n = 4–6 per group). B = *B. thermosphacta*, C = *C. maltaromaticum*; P = *P. fragi* and Lm = *L. monocytogenes*.

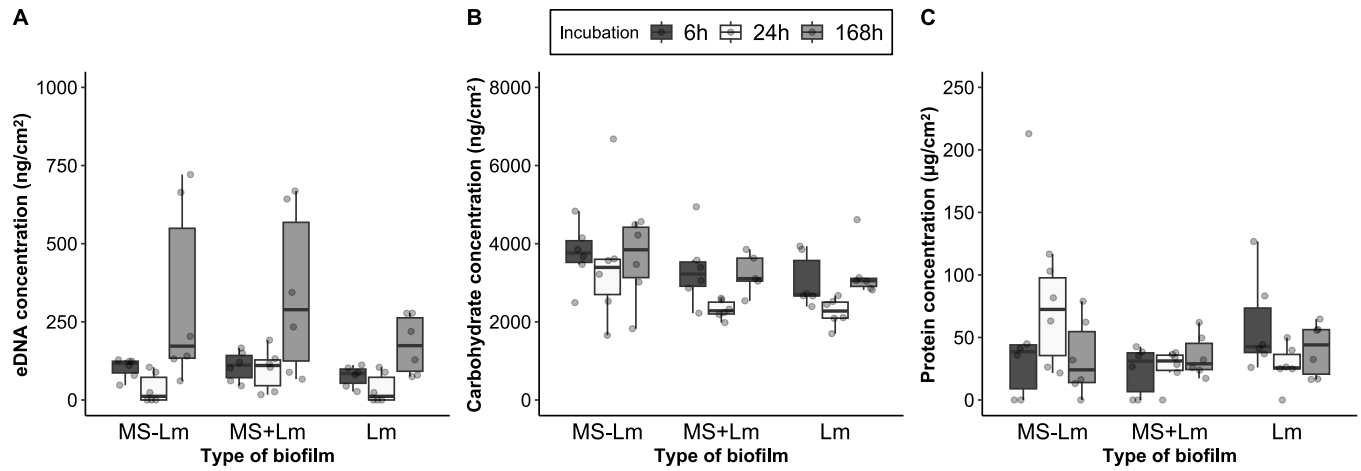

Fig. 6. Biofilm matrix. eDNA, carbohydrate (expressed as glucose equivalents) and protein load of the biofilm matrix within the different groups at the three time points are shown and given per cm^2. Samples with matrix values below the detection limit were completely excluded from the analysis. The indicated timepoints represents the time after (theoretical) *L. monocytogenes* addition. Multispecies biofilms were already incubated for 24 h (n at least 3 per group).

carbohydrate content of *Listeria*-only biofilms from 24 to 168 h (p-value = 0.026).

The highest mean load of proteins was detected after 6 h in the multispecies biofilm without *L. monocytogenes* (MS-Lm) (83.8 µg/cm^2) and the lowest protein amount was detected in the *Listeria* only biofilm after 24 hours (31.8 µg/cm^2). However, the protein content did neither significantly alter between the biofilms nor between the time points.

4. Discussion and outlook

In this study we explored the behaviour of *L. monocytogenes* in a simplified meat-related multispecies biofilm model. We selected this *L. monocytogenes* ST121 strain as it has colonised the production line of one company for at least one year (Stessl et al., 2020). ST121 strains are highly frequent in the FPE and are known to be able to persist for months and even years (Maury et al., 2016; Pasquali et al., 2018; Schmitz-Esser et al., 2015).

Bacteria need to attach to a surface and produce biofilm matrix to be able to build a biofilm. We used a genome-based approach for identifying potential biofilm-formation genes in the *B. thermosphacta*, *C. maltaromaticum*, *P. fragi* and *L. monocytogenes* strains. The search for biofilm associated features on the PATRIC database revealed that *P. fragi* harbours 21 genetic features potentially involved in biofilm lifestyle, whereas *B. thermosphacta* showed only one respective gene and *C. maltaromaticum* two (Wagner et al., 2021). The *L. monocytogenes* strain provided positive hits for one quorum sensing gene (*ytnP*), and 4 genes involved in teichoic acid production (one putative major teichoic acid biosynthesis protein C, *tagH*, *tagG* and *gtcA*). Teichonic acid is a commonly found matrix component of *L. monocytogenes* biofilms (Alonso et al., 2014). These findings indicate that this *L.* monocytogenes strain is able to produce diverse matrix components. We could confirm the attachment of *L. monocytogenes* on bare stainless steel surfaces already after 6 h of incubation, as well as the production of carbohydrates, eDNA and proteins. This indicates that the strain used is able to colonise stainless steel slides, however its biomass was very low at all time-points suggesting that *L. monocytogenes* alone does not build complex three-dimensional biofilms with high biomass yields. This is in accordance with literature (Doijad et al., 2015; Guilbaud et al., 2015), which showed that the majority of *L. monocytogenes* strains does not produce dense biofilms. According to the classification of Doijad et al. (2015) the strain used here is a weak biofilm former.

It is rather unlikely that *L. monocytogenes* monospecies biofilms exist outside the laboratory, therefore we focused on multispecies biofilms. We used strains from genera frequently associated with *Listeria*-positive sampling sites (*Pseudomonas*: (Diaz et al., 2025; Fox et al., 2014; Hascoët et al., 2019; Langsrud et al., 2016; Liu et al., 2016; Rodríguez-López et al., 2015); *Brochothrix*: (Diaz et al., 2025; Langsrud et al., 2016); *Carnobacterium*: (Diaz et al., 2025; Pracser et al., 2024; Rodríguez-López et al., 2020, 2019, 2015)). Within the meat sector the possible spoilage bacteria *Pseudomonas* spp., *Brochothrix thermosphacta* and *Carnobacterium maltaromaticum* have been isolated and described frequently (Maes et al., 2019; Odeyemi et al., 2020; Zwirzitz et al., 2021). Nevertheless, specific *C. maltaromaticum* strains have additionally been described as protective culture to inhibit spoilage and *L. monocytogenes* growth (Leisner et al., 2007).

L. monocytogenes behaviour in the multispecies biofilm was investigated by addition of a dense *L. monocytogenes* inoculum (6.7 log BCE/cm^2) to the 24 h old *B. thermosphacta-C. maltaromaticum-P. fragi* biofilms. Despite the low incubation temperatures (10 °C), *L. monocytogenes* was still able to colonise preexisting biofilms on stainless steel slides. It is a known feature of *L. monocytogenes* to be able to survive and grow at low temperatures (Osek et al., 2022). Puga et al. (2018) observed that colonisation of *L. monocytogenes* of *Pseudomonas fluorescens* biofilms was more efficient at cool temperatures (4 °C) compared to higher temperatures (20 °C). Furthermore, *L. monocytogenes* cells were multiplying, as observed by increasing cell numbers over time (6 h compared to 7 days) in both monospecies and multispecies growth conditions. Additionally, the relatively high number of RNAseq reads mapping to *L. monocytogenes* in the MS+Lm biofilm after 6 h reflects the active transcription in the multispecies community at low temperatures. To our knowledge our study is the first showing that *L. monocytogenes* is able to colonise preexisting biofilms. Several studies showed that *L. monocytogenes* was able to co-colonise polyvinyl chloride (PVC) and stainless steel surfaces with other bacteria resulting in complex multispecies biofilms (Fernández-Gómez et al., 2023; Lake et al., 2024). *P. fragi* was the most active player, accounting for 70 % and 80 % of total reads in the multispecies biofilm with and without *L. monocytogenes*. Despite showing similar cell numbers in the inoculum, *B. thermosphacta* and *C. maltaromaticum* showed reduced cell numbers (1.5 % and 1.1 %) and limited transcriptional activity in the biofilm.

The transcriptome analysis showed a higher expression of genes related to the flagellar assembly pathway (ko02040: *motA*, *motB*, *flgG*, *flhA*, *flhB*, *fliR*) in *L. monocytogenes* in the multispecies biofilm compared to the inoculum. These genes are part of diverse components of the flagella machinery (stator: *motA*, *motB* Rod, P/L ring, hook: *flgG*, MS/C ring, Type II secretion system (T3SS): *fliR*, and T3SS: *flhA*, *flhB*) (Osterman et al., 2015). Our data are in accordance with the study of Gou et al., which showed that the flagellar assembly pathway is one of

the top upregulated pathway in the biofilm at 12, 24 and 48 hours compared to the inoculum at 37 °C (Gou et al., 2023). Flagella and motility genes are known to be essential factors for successful biofilm formation of *L. monocytogenes* (Lemon et al., 2007). Furthermore, three among the top 20 over-expressed genes belonged to the pathway of bacterial chemotaxis (k02030: *motA*, *motB*, *cheV*), which is also in line with the study of Gou et al. (2023). Chemotaxis and motility are known to be involved in biofilm formation. Additionally, three genes related to the pathway "Two-component system" were upregulated (*motA, cheR and cheV*). Two-component systems have already been discussed to play a diverse role in biofilm formation (Alejandro-Navarreto and Freitag, 2024).

Further, several genes related to iron homeostasis were over-expressed (*srtB*, *ABC.FEV.S.*, *tatA*). Under iron deprivation conditions, sortase B (*srtB*) was highly expressed in *Staphylococcus aureus* (Geoghegan et al., 2010). This transpeptidase facilitates the processing and anchoring of surface proteins to the cell wall (Jose et al., 2023). The *ABC.FEV.S* gene encodes an iron complex transport system substrate-binding protein which is required for iron uptake. The twin-arginine translocase (tat) system is involved in iron uptake in *L. monocytogenes*. TatA was shown to be upregulated upon iron limitation (Ledala et al., 2010) under the regulation of the *fur* gene, which was also significantly upregulated in our data (1.65 log2 fold change). The upregulation of these iron-related genes in *L. monocytogenes* indicates iron-limited conditions; yet it has been shown that iron is needed for biofilm formation in *Klebsiella pneumoniae* and *Pseudomonas aeruginosa* (Chen et al., 2020; Kang and Kirienko, 2017).

The lack of differentially expressed genes between the MS+Lm and MS-Lm biofilm communities indicates a minimal perturbation by *L. monocytogenes* introduction. Interestingly, the increase in *C. maltaromaticum zntA* (cadmium/zinc exporting ATPase) in the multispecies biofilm where *L. monocytogenes* (MS+Lm*)* was present, suggests a perturbation of zinc homeostasis by *L. monocytogenes*. *ZntA* is present in numerous bacteria maintaining zinc homeostasis. Maunders et al. (2022) investigated this gene in *Klebsiella pneumoniae*. They concluded that biofilm formation contributes to the resistance against zinc stress potentially arising from a slower permeation or chelation of zinc ion diffusion facilitated by matrix components.

So far, transcription of *L. monocytogenes* at low temperatures has only been investigated in monospecies biofilms (Gray et al., 2021; 14°C) in an individual isolate comparison setup (i.e. 24 vs 48 h). After 24 h, Gray et al. showed that genes related to metabolism (PTS system, starch and sucrose, cobalamin biosynthesis) and prophage-related genes were significantly over-expressed. In line, our data showed five significantly up-regulated prophage genes in *L. monocytogenes* in the biofilms compared to the inoculum (*Phage_H_T_join*, *Phage_Gp23*, *DUF771*, *Phage-A118_gp45* and a phage integrase) and six downregulated (*phage holin family protein*, *YvIB*, *PspC domain-containing protein*, *phage tail proteins: Phage_TTP_1* and *Sipho_tail*; *DUF2479*) among the top 50 up- and down-DEGs. Prophages are often present in *L. monocytogenes*, where they have been shown to improve cell fitness and to act as complex virulence-associated molecular switches potentially allowing adaption mechanisms in the FPE (Argov et al., 2019; Verghese et al., 2011). The simultaneous up- and down-regulation of prophage genes highlights the complexity of prophages in *L. monocytogenes*. Numerous factors, especially stress (e.g. starvation, DNA damage or environmental stress), are known to induce prophages and activate lysogeny (Feiner et al., 2015). Our data suggest that *L. monocytogenes* is experiencing stress when colonising a multispecies biofilm, yet more studies are needed to explore the role of prophages in *L. monocytogenes* biofilm colonisation.

Our qPCR data indicate that the communities within the biofilms are not stable. After 24 h the cell numbers of all bacteria slightly increased in the multispecies biofilms. Yet, 7 days after the addition of *L. monocytogenes* (or 8 days of total incubation) there was an observable change in community composition and especially the relative numbers of *B. thermosphacta* and *C. maltaromaticum* increased. This is in line with a previous study showing an increase of *B. thermosphacta* and *C. maltaromaticum* cell numbers in complex biofilm communities after seven days (Fernández-Gómez et al., 2023). The presence of *L. monocytogenes* did not change the overall biofilm community structure. In the early timepoints (i.e. 6 h, 24 h) *L. monocytogenes* cell numbers were about one log higher in the multispecies biofilms compared to the only *L. monocytogenes* biofilm. This observation was previously done by Puga et al., (2018). They observed that *L. monocytogenes* colonisation numbers are 1–2 log higher when they grow on preformed biofilms compared to a bare surface. Similar observations can be drawn from our data after 6 and 24 h. Yet, after 7 days of incubation the bacterial load was comparable (0.3 log BCE difference).

We examined the basic matrix components eDNA, carbohydrates and proteins using quantitative detection methods, without qualitative analyses. As *L. monocytogenes* does not alter the multispecies biofilm community structure, it is not surprising that the biofilm basic matrix composition is not altered as well. If there are qualitative differences in the biofilm matrix remains to be determined. The amount of eDNA was comparable in the early timepoints (6 and 24 h), suggesting an important role of eDNA in initial attachment and the assurance of structural integrity, which has been previously described in different bacterial species (Tang et al., 2013) as well as *L. monocytogenes* (Harmsen et al., 2010; Zetzmann et al., 2015). Yet, at the late time-point (168 h), eDNA level drastically increased. This observation could be explained by the release of eDNA by lysed bacteria (Ibáñez de Aldecoa et al., 2017). In *L. monocytogenes* monospecies biofilms eDNA was described to gather in hollow voids, possible representing a potential food source for active cells (Colagiorgi et al., 2016; Guilbaud et al., 2015). The amount of carbohydrates (measured as glucose equivalents) was the lowest after 24 h of incubation. This could arise due to a remodelling of the biofilm matrix and synthesis of complex exopolysaccharides during the early phases of biofilm colonisation (Balducci et al., 2023). The protein amount in the biofilms' matrix was stable over all time points. It is known that proteins are essential for biofilm development and homeostasis enabling important emerging features of biofilms (Flemming and Wingender, 2010). Especially here a detailed analysis would be interesting, but this was beyond the scope of our study.

In a previous study, we explored the biofilm-forming ability of single strains from the meat processing environment, including the strains of *B. thermosphacta*, *C. maltaromaticum* and *P. fragi* from this study (Wagner et al., 2021). Despite using a similar experimental set-up, *B. thermosphacta* and *C. maltaromaticum* alone were not able to produce eDNA and proteins. Furthermore, a comparison of the data indicates that the combined effect of the individual strains does not correspond to the overall outcome observed in the multispecies biofilms, highlighting the complexity of bacterial interactions. Sadiq et al. (2024) have already shown in their detailed experiments with dual- three and four-species biofilms that bacterial interactions are highly diverse.

Our data show that the food-environmental *L. monocytogenes* isolate is able to colonise a pre-formed multispecies biofilm. Further, this study suggests that *L. monocytogenes* is residing within a multispecies biofilm, without altering the community structure or the overall matrix composition. This interesting observation could change our view on *L. monocytogenes* as an active player in the FPE to a passive survivor and resident of biofilms. Further research is needed to deepen our knowledge and understand the complex behaviour of *L. monocytogenes* in multispecies biofilms.

CRediT authorship contribution statement

Eva M. Voglauer: Writing – original draft, Visualization, Project administration, Methodology, Investigation, Formal analysis, Data curation, Conceptualization. **Lauren V. Alteio:** Writing – original draft, Visualization, Formal analysis, Data curation. **Narciso M. Quijada:** Writing – review & editing, Supervision. **Martin Wagner:** Writing –

review & editing, Resources, Funding acquisition. **Nadja Pracser:** Writing – review & editing. **Sarah Thalguter:** Writing – review & editing, Methodology. **Kathrin Rychli:** Writing – review & editing, Supervision, Conceptualization.

Declaration of Competing Interest

The author(s) declare no competing interests.

Acknowledgements

This work was created within a research project of the Austrian Competence Centre for Feed and Food Quality, Safety and Innovation (FFoQSI). The COMET-K1 competence centre FFoQSI is funded by the Austrian federal ministries BMK, BMDW and the Austrian provinces Lower Austria, Upper Austria and Vienna within the scope of COMET - Competence Centers for Excellent Technologies. The programme COMET is handled by the Austrian Research Promotion Agency FFG.

The authors acknowledge Bence Molnár for his technical support in growing and analysing seven-day old biofilms.

L.V.A is currently funded by the European Union's Horizon 2020 research and innovation programme under grant agreement no. 101060698.

N.M.Q. is currently funded by the European Union's Horizon 2020 research and innovation programme under the Marie Skłodowska-Curie grant agreement no. 101034371.

Appendix A. Supporting information

Supplementary data associated with this article can be found in the online version at doi:10.1016/j.micres.2024.127997.

Data availability

The sequenced data reported in this paper have been deposited in the National Center for Biotechnology Information Sequence Read Archive, (BioProject PRJNA1117023). The annotated *L. monocytogenes* genome was deposited in PATRIC under the genome ID: 1639.12587 and within NCBI under BioSample SAMN41725359. The *B. thermosphacta, C. maltaromaticum* and *P. fragi* sequences have been previously reported under PRJNA715602 (SRX10442542, SRX10442543, and SRX10442547, respectively).

References

Alejandro-Navarreto, X., Freitag, N.E., 2024. Revisiting old friends: updates on the role of two-component signaling systems in *Listeria monocytogenes* survival and pathogenesis. Infect. Immun. 92.

Alonso, A.N., Perry, K.J., Regeimbal, J.M., Regan, P.M., Higgins, D.E., 2014. Identification of *Listeria monocytogenes* determinants required for biofilm formation. PLoS One 9, 1–16. https://doi.org/10.1371/journal.pone.0113696.

Argov, T., Sapir, S.R., Pasechnek, A., Azulay, G., Stadnyuk, O., Rabinovich, L., Sigal, N., Borovok, I., Herskovits, A.A., 2019. Coordination of cohabiting phage elements supports bacteria–phage cooperation. Nat. Commun. 10. https://doi.org/10.1038/s41467-019-13296-x.

Armbruster, D.A., Pry, T., 2008. Limit of blank, limit of detection and limit of quantitation. Clin. Biochem. Rev. 29 (1), S49–S52.

Balducci, E., Papi, F., Capialbi, D.E., Del Bino, L., 2023. Polysaccharides' structures and functions in biofilm architecture of antimicrobial-resistant (AMR) pathogens. Int. J. Mol. Sci. 24. https://doi.org/10.3390/ijms24044030.

Belias, A., Sullivan, G., Wiedmann, M., Ivanek, R., 2022. Factors that contribute to persistent *Listeria* in food processing facilities and relevant interventions: A rapid review. Food Control 133, 108579. https://doi.org/10.1016/j.foodcont.2021.108579.

Blackman, I.C., Frank, J.F., Frank, F., 1996. Growth of *Listeria monocytogenes* as a biofilm on various food-processing surfaces. J. Food Prot. (8), 827–831. https://doi.org/10.4315/0362-028X-59.8.827.

Bokulich, N.A., Mills, D.A., 2013. Facility-specific "house" microbiome drives microbial landscapes of artisan cheesemaking plants. Appl. Environ. Microbiol. 79, 5214–5223. https://doi.org/10.1128/AEM.00934-13.

Bolger, A.M., Lohse, M., Usadel, B., 2014. Trimmomatic: a flexible trimmer for Illumina sequence data. Bioinformatics 30, 2114–2120. https://doi.org/10.1093/bioinformatics/btu170.

Buchfink, B., Reuter, K., Drost, H.G., 2021. Sensitive protein alignments at tree-of-life scale using DIAMOND. Nat. Methods 18, 366–368. https://doi.org/10.1038/s41592-021-01101-x.

Cámara, M., Green, W., MacPhee, C.E., Rakowska, P.D., Raval, R., Richardson, M.C., Slater-Jefferies, J., Steventon, K., Webb, J.S., 2022. Economic significance of biofilms: a multidisciplinary and cross-sectoral challenge. npj Biofilms Micro 8, 1–8. https://doi.org/10.1038/s41522-022-00306-y.

Carrascosa, C., Raheem, D., Ramos, F., Saraiva, A., Raposo, A., 2021. Microbial biofilms in the food industry—a comprehensive review. Int. J. Environ. Res. Public Health 18, 1–31. https://doi.org/10.3390/ijerph18042014.

Chen, T., Dong, G., Zhang, S., Zhang, X., Zhao, Y., Cao, J., Zhou, T., Wu, Q., 2020. Effects of iron on the growth, biofilm formation and virulence of *Klebsiella pneumoniae* causing liver abscess. BMC Microbiol 20, 1–7. https://doi.org/10.1186/s12866-020-01727-5.

Colagiorgi, A., Di Ciccio, P., Zanardi, E., Ghidini, S., Ianieri, A., 2016. A look inside the *Listeria monocytogenes* biofilms extracellular matrix. Microorganisms 4, 22. https://doi.org/10.3390/microorganisms4030022.

Diaz, M., Aird, H., Le Viet, T., Gutiérrez, A.V., Larke-Mejia, N., Omelchenko, O., Moragues-Solanas, L., Fritscher, J., Som, N., McLauchlin, J., Hildebrand, F., Jørgensen, F., Gilmour, M., 2025. Microbial composition and dynamics in environmental samples from a ready-to-eat food production facility with a long-term colonization of *Listeria monocytogenes*. Food Microbiol 125. https://doi.org/10.1016/j.fm.2024.104649.

Dixon, E., Rabanser, I., Dzieciol, M., Zwirzitz, B., Wagner, M., Mann, E., Stessl, B., Wetzels, S.U., 2019. Reduction potential of steam vacuum and high-pressure water treatment on microbes during beef meat processing. Food Control 106, 106728. https://doi.org/10.1016/j.foodcont.2019.106728.

Doijad, S.P., Barbuddhe, S.B., Garg, S., Poharkar, K.V., Kalorey, D.R., Kurkure, N.V., Rawool, D.B., Chakraborty, T., 2015. Biofilm-forming abilities of *Listeria monocytogenes* serotypes isolated from different sources. PLoS One 10, 1–14. https://doi.org/10.1371/journal.pone.0137046.

Fagerlund, A., Langsrud, S., Møretrø, T., 2021. Microbial diversity and ecology of biofilms in food industry environments associated with *Listeria monocytogenes* persistence. Curr. Opin. Food Sci. 37, 171–178. https://doi.org/10.1016/j.cofs.2020.10.015.

Fagerlund, A., Langsrud, S., Schirmer, B.C.T., Møretrø, T., Heir, E., 2016. Genome analysis of *Listeria monocytogenes* sequence type 8 strains persisting in salmon and poultry processing environments and comparison with related strains. PLoS One 11, 1–22. https://doi.org/10.1371/journal.pone.0151117.

Feiner, R., Argov, T., Rabinovich, L., Sigal, N., Borovok, I., Herskovits, A.A., 2015. A new perspective on lysogeny: Prophages as active regulatory switches of bacteria. Nat. Rev. Microbiol. 13, 641–650. https://doi.org/10.1038/nrmicro3527.

Fernández-Gómez, P., Oliveira, M., Cobo-Díaz, J.F., González-Raurich, M., Múgica-Vidal, R., Alba-Elías, F., Prieto, M., Alvarez-Ordóñez, A., López, M., 2023. The background microbiota and sanitization agent drive the fate of *Listeria monocytogenes* in multispecies biofilms formed on a plasma-polymerized coating applied on stainless steel. Int. J. Food Microbiol. 386. https://doi.org/10.1016/j.ijfoodmicro.2022.110017.

Flemming, H.C., van Hullebusch, E.D., Neu, T.R., Nielsen, P.H., Seviour, T., Stoodley, P., Wingender, J., Wuertz, S., 2022. The biofilm matrix: multitasking in a shared space, 0123456789 Nat. Rev. Microbiol.. https://doi.org/10.1038/s41579-022-00791-0.

Flemming, H.-C., Wingender, J., 2010. The biofilm matrix. Nat. Rev. Microbiol. 8, 623–633. https://doi.org/10.1080/0892701031000072190.

Flemming, H.-C., Wingender, J., Szewzyk, U., Steinberg, P., Rice, S.A., Kjelleberg, S., 2016. Biofilms: an emergent form of bacterial life. Nat. Rev. Microbiol. 14, 563–575. https://doi.org/10.1038/nrmicro.2016.94.

Food-Borne Disease Burden Epidemiology Reference Group 2007-2015, 2015. WHO estamates of the global burden of foodborn diseases, WHO Library Cataloguing-in-Publication Data. World Health Organization, Berlin, Heidelberg. https://doi.org/10.1007/978-3-662-43978-4_3884.

Fox, E.M., Solomon, K., Moore, J.E., Wall, P.G., Fanning, S., 2014. Phylogenetic profiles of in-house microflora in drains at a food production facility: comparison and biocontrol implications of *Listeria*-positive and -negative bacterial populations. Appl. Environ. Microbiol. 80, 3369–3374. https://doi.org/10.1128/AEM.00468-14.

Geoghegan, J.A., Corrigan, R.M., Gruszka, D.T., Speziale, P., O'Gara, J.P., Potts, J.R., Foster, T.J., 2010. Role of surface protein SasG in biofilm formation by *Staphylococcus aureus*. J. Bacteriol. 192, 5663–5673. https://doi.org/10.1128/JB.00628-10.

Giaouris, E.E., Simões, M. V, 2018. Pathogenic biofilm formation in the food industry and alternative control strategies, in: Foodborne Diseases. pp. 309–377. https://doi.org/10.1016/B978-0-12-811444-5.00011-7.

Gou, H., Cao, Q., Wang, Z., Liu, Y., Sun, Y., Wei, H., Song, C., Tian, C., Wei, Y., Xue, H., 2023. Transcriptomic analysis of *Listeria monocytogenes* biofilm formation at different times. Can. J. Vet. Res. 87, 59–66.

Gray, J., Chandry, P.S., Kaur, M., Kocharunchitt, C., Fanning, S., Bowman, J.P., Fox, E. M., 2021. Colonisation dynamics of *Listeria monocytogenes* strains isolated from food production environments. Sci. Rep. 11, 1–17. https://doi.org/10.1038/s41598-021-91503-w.

Guilbaud, M., Piveteau, P., Desvaux, M., Brisse, S., Briandet, R., 2015. Exploring the diversity of *Listeria monocytogenes* biofilm architecture by high-throughput confocal laser scanning microscopy and the predominance of the honeycomb-like morphotype. Appl. Environ. Microbiol. 81, 1813–1819. https://doi.org/10.1128/AEM.03173-14.

Gurevich, A., Saveliev, V., Vyahhi, N., Tesler, G., 2013. QUAST: quality assessment tool for genome assemblies. Genome Anal. 29, 1072–1075. https://doi.org/10.1093/bioinformatics/btt086.

Harmsen, M., Lappann, M., Knøchel, S., Molin, S., 2010. Role of extracellular DNA during biofilm formation by *Listeria monocytogenes*. Appl. Environ. Microbiol. 76, 2271–2279. https://doi.org/10.1128/AEM.02361-09.

Harrand, A.S., Jagadeesan, B., Baert, L., Wiedmann, M., Orsi, R.H., 2020. Evolution of *Listeria monocytogenes* in a food processing plant involves limited single-nucleotide substitutions but considerable diversification by gain and loss of prophages. Appl. Environ. Microbiol. 86. https://doi.org/10.1128/AEM.02493-19.

Hascoët, A.S., Ripolles-Avila, C., Guerrero-Navarro, A.E., Rodríguez-Jerez, J.J., 2019. Microbial ecology evaluation of an Iberian pig processing plant through implementing SCH sensors and the influence of the resident microbiota on*Listeria monocytogenes*. Appl. Sci. 9, 1–14. https://doi.org/10.3390/app9214611.

Huerta-Cepas, J., Szklarczyk, D., Heller, D., Hernández-Plaza, A., Forslund, S.K., Cook, H., Mende, D.R., Letunic, I., Rattei, T., Jensen, L.J., Von Mering, C., Bork, P., 2018. eggNOG 5.0: a hierarchical, functionally and phylogenetically annotated orthology resource based on 5090 organisms and 2502 viruses. Nucleic Acids Res 47, 309–314. https://doi.org/10.1093/nar/gky1085.

Ibáñez de Aldecoa, A.L., Zafra, O., González-Pastor, J.E., 2017. Mechanisms and regulation of extracellular DNA release and its biological roles in microbial communities. Front. Microbiol. 8, 1–19. https://doi.org/10.3389/fmicb.2017.01390.

Jose, S., Terrero-Salcedo, D., Madan, R., 2023. *Clostridioides difficile*: from "difficult to grow" to "difficult to treat. (Third Ed.). Mol. Med. Microbiol. 945–956. https://doi.org/10.1016/B978-0-12-818619-0.00146-5.

Kanehisa, M., Sato, Y., Kawashima, M., Furumichi, M., Tanabe, M., 2015. KEGG as a reference resource for gene and protein annotation. Nucleic Acids Res 44, 457–462. https://doi.org/10.1093/nar/gkv1070.

Kang, D., Kirienko, N.V., 2017. Interdependence between iron acquisition and biofilm formation in *Pseudomonas aeruginosa*. J. Microbiol. 56, 100–106. https://doi.org/10.1177/0022146515594631.Marriage.

Kassambara, A., 2023. ggpubr: "ggplot2" Based Publication Ready Plots.

Kopylova, E., Noé, L., Touzet, H., 2012. SortMeRNA: Fast and accurate filtering of ribosomal RNAs in metatranscriptomic data. Bioinformatics. https://doi.org/10.1093/bioinformatics/bts611.

Kubota, H., Senda, S., Nomura, N., Tokuda, H., Uchiyama, H., 2008. Biofilm formation by lactic acid bacteria and resistance to environmental stress. J. Biosci. Bioeng. 106, 381–386. https://doi.org/10.1263/jbb.106.381.

Lake, F.B., Chen, J., van Overbeek, L.S., Baars, J.J.P., Abee, T., den Besten, H.M.W., 2024. Biofilm formation and desiccation survival of *Listeria monocytogenes* with microbiota on mushroom processing surfaces and the effect of cleaning and disinfection. Int. J. Food Microbiol. 411, 110509. https://doi.org/10.1016/j.ijfoodmicro.2023.110509.

Langmead, B., Salzberg, S., 2012. Fast gapped-read alignment with Bowtie 2. Nat. Methods 9, 357–359.

Langsrud, S., Moen, B., Møretrø, T., Løype, M., Heir, E., 2016. Microbial dynamics in mixed culture biofilms of bacteria surviving sanitation of conveyor belts in salmon-processing plants. J. Appl. Microbiol. 120, 366–378. https://doi.org/10.1111/jam.13013.

Ledala, N., Sengupta, M., Muthaiyan, A., Wilkinson, B.J., Jayaswal, R.K., 2010. Transcriptomic response of *Listeria monocytogenes* to iron limitation and fur mutation. Appl. Environ. Microbiol. 76, 406–416. https://doi.org/10.1128/AEM.01389-09.

Leisner, J.J., Laursen, B.G., Prévost, H., Drider, D., Dalgaard, P., 2007. *Carnobacterium*: Positive and negative effects in the environment and in foods. FEMS Microbiol. Rev. 31, 592–613. https://doi.org/10.1111/j.1574-6976.2007.00080.x.

Lemon, K.P., Higgins, D.E., Kolter, R., 2007. Flagellar motility is critical for *Listeria monocytogenes* biofilm formation. J. Bacteriol. 189, 4418–4424. https://doi.org/10.1128/JB.01967-06.

Liao, Y., Smyth, G.K., Shi, W., 2014a. Sequence analysis featureCounts: an efficient general purpose program for assigning sequence reads to genomic features 30, 923–930. https://doi.org/10.1093/bioinformatics/btt656.

Liao, Y., Smyth, G.K., Shi, W., 2014b. featureCounts: an efficient general purpose program for assigning sequence reads to genomic features. Bioinformatics 30, 923–930. https://doi.org/10.1093/bioinformatics/btt656.

Liu, Y., Zhang, H., Wu, C., Deng, W., Wang, D., Zhao, G., Song, J., Jiang, Y., 2016. Molecular analysis of dominant species in *Listeria monocytogenes*-positive biofilms in the drains of food processing facilities. Appl. Microbiol. Biotechnol. 100, 3165–3175. https://doi.org/10.1007/s00253-015-7203-z.

Love, M., Anders, W., 2014. Moderated estimation of fold change and dispersion for RNA-seq data with DESeq2. Genome Biol. 15. https://doi.org/10.1186/s13059-014-0550-8.

Luo, W., Friedman, M.S., Shedden, K., Hankenson, K.D., Woolf, P.J., 2009. GAGE: generally applicable gene set enrichment for pathway analysis. BMC Bioinforma. 10, 161. https://doi.org/10.1186/1471-2105-10-161.

Maes, S., Heyndrickx, M., Vackier, T., Steenackers, H., Verplaetse, A., De Reu, K., 2019. Identification and spoilage potential of the remaining dominant microbiota on food contact surfaces after cleaning and disinfection in different food industries. J. Food Prot. 82, 262–275. https://doi.org/10.4315/0362-028X.JFP-18-226.

Maes, S., Huu, S.N., Heyndrickx, M., Weyenberg, S.Van, Steenackers, H., Verplaetse, A., Vackier, T., Sampers, I., Raes, K., De Reu, K., 2017. Evaluation of two surface sampling methods for microbiological and chemical analyses to assess the presence of biofilms in food companies. J. Food Prot. 80, 2022–2028. https://doi.org/10.4315/0362-028X.JFP-17-210.

Mah, T.F.C., O'Toole, G.A., 2001. Mechanisms of biofilm resistance to antimicrobial agents. Trends Microbiol 9, 34–39. https://doi.org/10.1016/S0966-842X(00)01913-2.

Maunders, E.A., Ganio, K., Hayes, A.J., Neville, S.L., Davies, M.R., Strugnell, R.A., McDevitt, C.A., Tan, A., 2022. The role of ZntA in *Klebsiella pneumoniae* zinc homeostasis. Microbiol. Spectr. 10. https://doi.org/10.1128/spectrum.01773-21.

Maury, M.M., Tsai, Y.-H., Charlier, C., Touchon, M., Chenal-Francisque, V., Leclercq, A., Criscuolo, A., Gaultier, C., Roussel, S., Brisabois, A., Disson, O., Rocha, E.P.C., Brisse, S., Lecuit, M., 2016. Uncovering *Listeria monocytogenes* hypervirulence by harnessing its biodiversity. Nat. Genet. 48, 308–313. https://doi.org/10.1038/ng.3501.

Odeyemi, O.A., Alegbeleye, O.O., Strateva, M., Stratev, D., 2020. Understanding spoilage microbial community and spoilage mechanisms in foods of animal origin. Compr. Rev. Food Sci. Food Saf. 19, 311–331. https://doi.org/10.1111/1541-4337.12526.

Osek, J., Lachtara, B., Wieczorek, K., 2022. *Listeria monocytogenes* – How this pathogen survives in food-production environments? Front. Microbiol. 13, 1–21. https://doi.org/10.3389/fmicb.2022.866462.

Osterman, I.A., Dikhtyar, Y.Y., Bogdanov, A.A., Dontsova, O.A., Sergiev, P.V., 2015. Regulation of flagellar gene expression in bacteria. Biochem 80, 1447–1456. https://doi.org/10.1134/S000629791511005X.

Pasquali, F., Palma, F., Guillier, L., Lucchi, A., Cesare, A., De, Manfreda, G., 2018. *Listeria monocytogenes* sequence types 121 and 14 repeatedly isolated within one year of sampling in a rabbit meat processing plant: Persistence and ecophysiology. Front. Microbiol. 9, 1–12. https://doi.org/10.3389/fmicb.2018.00596.

Pracser, N., Voglauer, E.M., Thalguter, S., Pietzka, A., Selberherr, E., Wagner, M., Rychli, K., 2024. Exploring the occurrence of *Listeria* in biofilms and deciphering the bacterial community in a frozen vegetable producing environment. Front. Microbiol. 15. https://doi.org/10.3389/fmicb.2024.1404002.

Puga, C.H., Dahdouh, E., SanJose, C., Orgaz, B., 2018. *Listeria monocytogenes* colonizes *Pseudomonas fluorescens* biofilms and induces matrix over-production. Front. Microbiol. 9, 1–12. https://doi.org/10.3389/fmicb.2018.01706.

Quijada, N.M., Mann, E., Wagner, M., Rodríguez-Lázaro, D., Hernández, M., Schmitz-Esser, S., 2018. Autochthonous facility-specific microbiota dominates washed-rind Austrian hard cheese surfaces and its production environment. Int. J. Food Microbiol. 267, 54–61. https://doi.org/10.1016/j.ijfoodmicro.2017.12.025.

R Core Team, 2020. R: A language and environment for statistical computing. ⟨https://www.r-project.org/⟩.

Rieu, A., Briandet, R., Habimana, O., Garmyn, D., Guzzo, J., Piveteau, P., 2008. *Listeria monocytogenes* EGD-e biofilms: No mushrooms but a network of knitted chains. Appl. Environ. Microbiol. 74, 4491–4497. https://doi.org/10.1128/AEM.00255-08.

Rodríguez-López, P., Bernárdez, M., Rodríguez-Herrera, J.J., Comesaña, Á.S., Cabo, M.L., 2019. Identification and metagenetic characterisation of *Listeria monocytogenes*-harbouring communities present in food-related industrial environments. Food Control 95, 6–17. https://doi.org/10.1016/j.foodcont.2018.07.023.

Rodríguez-López, P., Rodríguez-Herrera, J.J., Cabo, M.L., 2020. Tracking bacteriome variation over time in *Listeria monocytogenes*-positive foci in food industry. Int. J. Food Microbiol. 315, 108439. https://doi.org/10.1016/j.ijfoodmicro.2019.108439.

Rodríguez-López, P., Saá-Ibusquiza, P., Mosquera-Fernández, M., López-Cabo, M., López-Cabo a, M., 2015. *Listeria monocytogenes*-carrying consortia in food industry. Composition, subtyping and numerical characterisation of mono-species biofilm dynamics on stainless steel. Int. J. Food Microbiol. 206, 84–95. https://doi.org/10.1016/j.ijfoodmicro.2015.05.003.

Rolon, M.L., Voloshchuk, O., Bartlett, K.V., Laborde, L.F., Kovac, J., 2024. Biofilm Multi-species biofilms of environmental microbiota isolated from fruit packing facilities promoted tolerance of *Listeria monocytogenes* benzalkonium chloride. Biofilm 7, 100177. https://doi.org/10.1016/j.bioflm.2024.100177.

Rossmanith, P., Krassnig, M., Wagner, M., Hein, I., 2006. Detection of *Listeria monocytogenes* in food using a combined enrichment/real-time PCR method targeting the *prfA* gene. Res. Microbiol. 157, 763–771. https://doi.org/10.1016/j.resmic.2006.03.003.

Rychli, K., Grunert, T., Ciolacu, L., Zaiser, A., Razzazi-Fazeli, E., Schmitz-Esser, S., Ehling-Schulz, M., Wagner, M., 2016. Exoproteome analysis reveals higher abundance of proteins linked to alkaline stress in persistent *Listeria monocytogenes* strains. Int. J. Food Microbiol. 218, 17–26. https://doi.org/10.1016/j.ijfoodmicro.2015.11.002.

Sadiq, F.A., De Reu, K., Yang, N., Burmølle, M., Heyndrickx, M., 2024. Interspecies interactions in dairy biofilms drive community structure and response against cleaning and disinfection. Biofilm 7. https://doi.org/10.1016/j.bioflm.2024.100195.

Schmitz-Esser, S., Müller, A., Stessl, B., Wagner, M., 2015. Genomes of sequence type 121 *Listeria monocytogenes* strains harbor highly conserved plasmids and prophages. Front. Microbiol. 6. https://doi.org/10.3389/fmicb.2015.00380.

Stessl, B., Szakmary-Brändle, K., Vorberg, U., Schoder, D., Wagner, M., 2020. Temporal analysis of the *Listeria monocytogenes* population structure in floor drains during reconstruction and expansion of a meat processing plant. Int. J. Food Microbiol. 314, 108360. https://doi.org/10.1016/j.ijfoodmicro.2019.108360.

Tang, L., Schramm, A., Neu, T.R., Revsbech, N.P., Meyer, R.L., 2013. Extracellular DNA in adhesion and biofilm formation of four environmental isolates: A quantitative study. FEMS Microbiol. Ecol. 86, 394–403. https://doi.org/10.1111/1574-6941.12168.

Truelstrup Hansen, L., Vogel, B.F., 2011. Desiccation of adhering and biofilm *Listeria monocytogenes* on stainless steel: survival and transfer to salmon products. Int. J. Food Microbiol. 146, 88–93. https://doi.org/10.1016/j.ijfoodmicro.2011.01.032.

Verghese, B., Lok, M., Wen, J., Alessandria, V., Chen, Y., Kathariou, S., Knabel, S., 2011. *comK* prophage junction fragments as markers for *Listeria monocytogenes* genotypes unique to individual meat and poultry processing plants and a model for rapid niche-

specific adaptation, biofilm formation, and persistence. Appl. Environ. Microbiol. 77, 3279–3292. https://doi.org/10.1128/AEM.00546-11.
Wagner, E.M., Fischel, K., Rammer, N., Beer, C., Palmetzhofer, A.L., Conrady, B., Roch, F., Hanson, B.T., Wagner, M., Rychli, K., 2021. Bacteria of eleven different species isolated from biofilms in a meat processing environment have diverse biofilm forming abilities. Int. J. Food Microbiol. 349, 109232. https://doi.org/10.1016/j.ijfoodmicro.2021.109232.
Wagner, E.M., Pracser, N., Thalguter, S., Fischel, K., Rammer, N., Pospíšilová, L., Alispahic, M., Wagner, M., Rychli, K., 2020. Identification of biofilm hotspots in a meat processing environment: Detection of spoilage bacteria in multi-species biofilms. Int. J. Food Microbiol. 328, 108668. https://doi.org/10.1016/j.ijfoodmicro.2020.108668.
Wickham, H., 2016. ggplot2: Elegant Graphics for Data Analysis.
Xiao, N., 2024. ggsci: Scientific Journal and Sci-Fi Themed Color Palettes for "ggplot2."
Xu, Z.S., Ju, T., Yang, X., Gänzle, M., 2023. A meta-analysis of bacterial communities in food processing facilities: Driving forces for assembly of core and accessory microbiomes across different food commodities. Microorganisms 11, 1575. https://doi.org/10.3390/microorganisms11061575.
Zetzmann, M., Okshevsky, M., Endres, J., Sedlag, A., Caccia, N., Auchter, M., Waidmann, M.S., Desvaux, M., Meyer, R.L., Riedel, C.U., 2015. DNase-sensitive and -resistant modes of biofilm formation by *Listeria monocytogenes*. Front. Microbiol. 6, 1–11. https://doi.org/10.3389/fmicb.2015.01428.
Zwirzitz, B., Wetzels, S.U., Dixon, E.D., Stessl, B., Zaiser, A., Rabanser, I., Thalguter, S., Pinior, B., Roch, F.F., Strachan, C., Zanghellini, J., Dzieciol, M., Wagner, M., Selberherr, E., 2020. The sources and transmission routes of microbial populations throughout a meat processing facility. npj Biofilms Micro 6, 1–12. https://doi.org/10.1038/s41522-020-0136-z.
Zwirzitz, B., Wetzels, S.U., Dixon, E.D., Fleischmann, S., Selberherr, E., Thalguter, S., Quijada, N.M., Dzieciol, M., Stessl, B., 2021. Co-occurrence of *Listeria* spp. and spoilage associated microbiota during meat processing due to cross-contamination events. Front. Microbiol. 12. https://doi.org/10.3389/fmicb.2021.632935.